Ultrasensitive lateral flow assay to detect ribonuclease using quantum dots

Braden Oddo, Luke Ford, Lance P. Ford, Joseph F. Krebs†

Attogene, Inc. 3913 Todd Lane Suite 310 Austin TX 78744

† Corresponding author: jkrebs@attogene.com

Introduction

Recent innovations in RNA technology, including improved RNA design, manufacturing, and delivery systems have significantly increased the efficacy and stability of mRNA-based therapies [1, 2]. These advancements have led to remarkable advances in their safety and efficacy, making mRNA a promising platform for numerous therapeutic applications [3]. The remarkable success of mRNA COVID-19 vaccines has demonstrated the immense potential of RNA technology and sparked a surge in research and development, focusing on vaccines, therapeutics, and diagnostic tools for human diseases [4]. RNA researchers and pharmaceutical companies are actively exploring the vast potential of mRNAs to address a wide range of unmet medical needs. Universities across the nation are fueling the continual discovery of new tools to create
to manufacture and deliver novel biologically active RNAs. Pharmaceutical companies have experienced rapid growth in recent years and are expanding their RNA-based pipelines to develop vaccines [4]. To keep up with this, other pharmaceutical companies are investing heavily in RNA technologies to drive their vaccines and therapeutic programs. Drug companies are now i) expanding their RNA vaccine pipelines to create vaccines for other infectious diseases such as HIV, influenza, and malaria [5]; ii) exploring RNA-based therapeutics to treat diseases, including cancer [6], autoimmune diseases, and genetic disorders [7]; and iii) improving delivery systems to enhance the stability, safety, and efficacy of RNAs [8]. These concerted efforts will inevitably lead to the development and commercialization of new drugs and vaccines that can improve our health in ways that were previously unimaginable using traditional protein and small-molecule tools.

The structural integrity of RNA is vital for its functional activity and remains a significant challenge in the development of RNA-based vaccines and therapies [9, 10]. Quality Control is and will remain fundamental to the continued growth and maturation of the therapeutic RNA market [11, 12]. To ensure the safety and efficacy of RNA-based therapeutics, it is crucial to continually update and standardize the quality standards and control systems [12]. This is especially true in the rapidly growing biobanking field, where there is an industry-wide movement to standardize RNA sample processing and quality measurement [13 -16]. Given the unique characteristics of RNA and the complexity of mRNA-based products, specialized manufacturing and handling methods are essential for RNA vaccines and therapeutics [17]. Robust and consistent quality management systems must be adapted to meet these critical needs [12, 18].

Working with RNA is quite demanding due to the chemical instability of RNA and the ubiquitous presence of ribonucleases (RNases), which efficiently cleave and degrade RNA [19, 20]. RNases are exceedingly stable enzymes [21, 22]. RNases such as RNase A are found everywhere, including in equipment, hard surfaces, and airborne particles [22]. RNase contamination can have detrimental effects on valuable RNA [17]. All RNA manufacturers, curators, and researchers, including those in Bioprocessing, Biomanufacturing, Biobanking, and Life Science research areas, must take special precautions to limit the risk of RNase contamination risk [23-27]. These precautions include working in dedicated RNase-free areas and wearing gloves, lab coats, hair, and foot protection. It is also important to treat benchtop surfaces and glassware/plasticware with RNase-inactivating agents such as RNaseZap.

Despite stringent precautions, contamination can occur in any laboratory setting. Pharmaceutical companies, biobanks and university research labs must implement Quality Control measures at multiple levels in their workflows [17, 23, 28]. These measures include sensitive, robust, and consistent RNase testing [22]. Routine screening of the work environment, reagents, and products is essential to effectively manage and control the introduction of unwanted RNases. Unfortunately, current methods for detecting RNase contamination can be highly variable between laboratories and often require subjective interpretation of the results. Materials can be monitored using traditional “homebrew” RNase detection methods such as capillary gel electrophoresis [22], electrophoretic zymograms [29, 30], methylene blue [31], radiolabeling assays [32],

electrochemical [33, 34], and commercial FRET-based assay systems such as RNaseAlert [35]. These methods have numerous drawbacks: (i) they are time-consuming and often take many hours to complete, (ii) they produce inconsistent, subjective results requiring user interpretation, and (iii) they lack the traceability, standardization, and consistency required for QMS-focused organizations. In addition, these tests require (iv) hazardous radiation, (v) complicated procedures, and (vi) expensive equipment that can vary in detection sensitivity [36].

Lateral flow assays (LFAs) possess unique characteristics that make them well-suited for the detection of nucleases throughout the work environment. One of the primary benefits is their rapid and real-time detection capability [37]. LFAs can provide results within minutes, allowing immediate intervention if nuclease contamination is detected, thereby minimizing the potential damage to mRNA integrity. This quick turnaround is crucial in a high-throughput production environment, where time is essential. In addition, LFAs are user-friendly and require minimal training. Their straightforward design makes them accessible to a wide range of personnel, reducing the need for specialized training and complex laboratory equipment. This ease of use also translates to cost savings, as the assays are relatively inexpensive compared to other nucleic acid detection methods, such as PCR or next-generation sequencing. Finally, LFAs are portable and do not require sophisticated infrastructure. This portability allows on-site testing in different areas of production facilities, enabling continuous monitoring and ensuring that any contamination is promptly identified and addressed.

Quantum dots (Qdots) are versatile fluorescent nanoparticles that are used for the labeling and detection of biomolecules. Qdots contain a core containing a mixture of a semiconductor metals, such as selenium and cadmium, coated with a shell of ZnS or other materials to efficiently capture incoming photons. Qdots are often coated with a polymer to permit chemical derivatization for use as biosensors. Qdots are highly efficient particles for generating fluorescence; their intrinsic brightness is often many times that of other types of fluorophores. The surface of the Qdots can be readily derivatized to facilitate attachment to antibodies or affinity tags to produce highly stable and detectable reagents for lateral flow tests [38]. For example, a carboxylate-derivatized Qdot surface can be stably coated with antibodies or streptavidin using carbodiimide to permit binding of biotin and biotin conjugates. Lateral flow assays utilizing Qdot-based detection exhibit greater sensitivity than those utilizing colloidal gold or traditional chemical fluorophores [39-42].

We developed an ultrasensitive, easy-to-use quantum dot-based lateral flow assay system to detect RNase contamination in manufacturing environments and supply chain components. Our system, described in this publication, has unsurpassed speed and sensitivity, providing a means to proactively prevent RNase contamination issues before they occur, as well as to troubleshoot RNase problems in solutions and surfaces to rapidly solve problems when they arise.

Assay principle

Our test utilizes RNA oligonucleotides coupled to highly fluorescent quantum dots on one end (via biotin) and an affinity tag such as fluorescein (FAM) or digoxigenin (DIG). Intact RNA permits the quantum dots to be tethered to the test line, thus producing a strong test line signal when RNase is absent from a test sample (Figure 1). These oligonucleotides can be mixed with liquid samples and applied to sample pads at the end of a nitrocellulose membrane strip. Oligonucleotides can bind to both the test line and the control line as they flow up the strip, creating a two-line fluorescent signal.

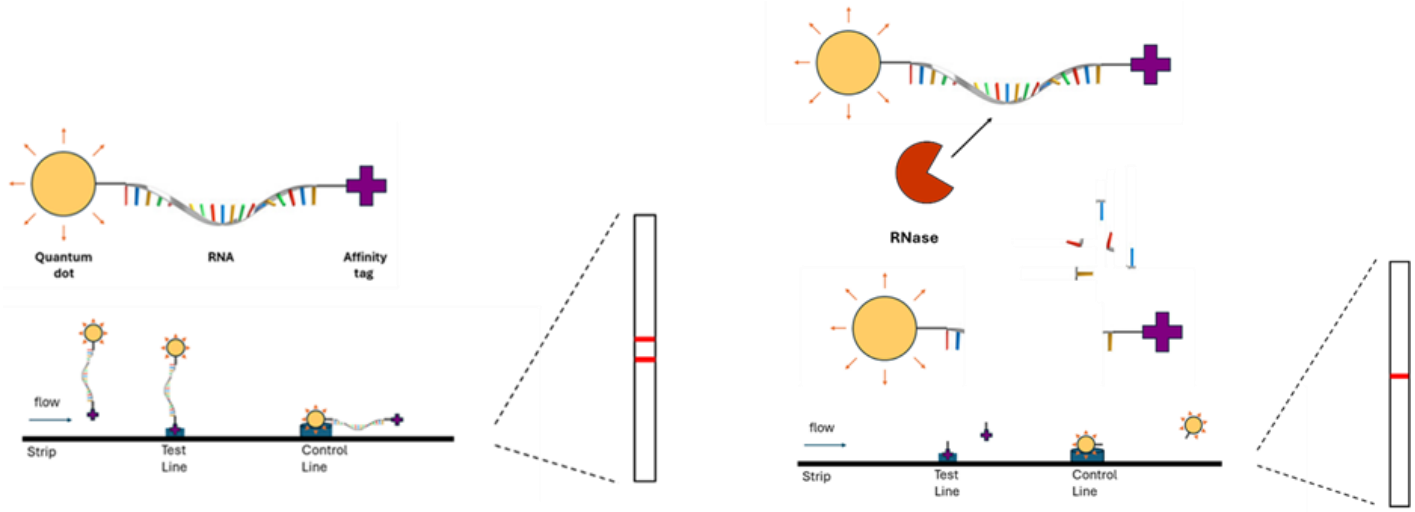

Figure 1. Qdot-based lateral flow device to detect RNase using dual-labeled oligonucleotides. After incubating the FAM/biotin RNA oligonucleotide with the sample, it is mixed with Qdots, which bind to the oligonucleotides, and then applied to the sample pad. The Qdots are coated with a DNA oligonucleotide that always binds to the control line. As the sample flows up the strip, the Qdots contact and bind to immobilized anti-FAM and anti-DIG antibodies, forming the test and control lines, respectively. Left. If the sample lacks RNase, then the intact RNA oligonucleotide causes the Qdots to bind to both lines, resulting in a strip with two fluorescent lines. Right. If the sample contains RNase, the enzyme cleaves the RNA substrate, preventing the Qdots from binding to the test line. Consequently, the test strip will show only one fluorescent (control) line.

Results

Detection of intact RNA oligonucleotides using a lateral flow assay

When a liquid sample containing the oligonucleotide-coated Qdots flows through the nitrocellulose test strip, the FAM-labeled RNA oligonucleotide can bind to the test line containing the immobilized anti-FAM antibody, thereby tethering the Qdot at the line. The immobilized Qdots formed a bright fluorescent test line on the strip. (Figure 2). The fluorescence intensity of the test line is visually observable using a UV lamp or can be quantified using a fluorescence strip reader, such as the Nanostrip Viewer from Nanohmics. The DIG/biotin-labeled DNA oligonucleotide was also coated onto the Qdots, allowing a portion of the nanoparticles to bind to the control line (anti-DIG). The control line signal was used to normalize the assay and to confirm adequate liquid flow through the strip.

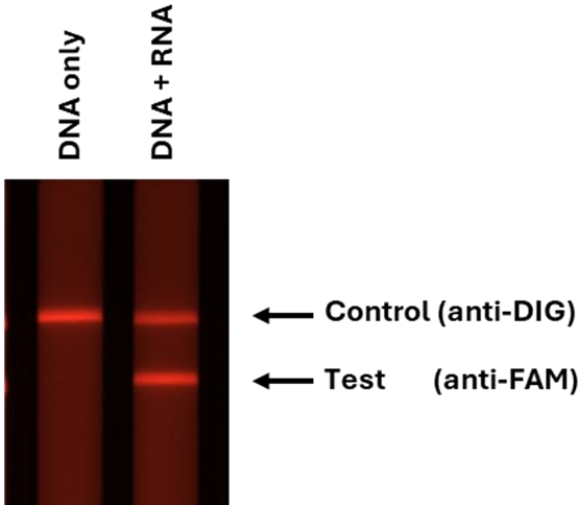

Figure 2. Fluorescent signal produced by oligonucleotide binding of Qdots to test line of lateral flow strip. Mixing the Qdots with DIG/Biotin labeled DNA allows them to bind to the control line as they flow up the strip, causing a fluorescent signal at the control line (left and right strips). If the Qdots are also mixed with the FAM/biotin RNA, they also bind to the test line (right strip). The positions of the control and test lines are indicated by the arrows.

Sensitive detection of ribonuclease using lateral flow with a fluorescence strip reader

Preincubation of the 17-mer RNA oligonucleotide (17 mer) with 0.5 picograms ribonuclease A in a buffered solution, such as 50 mM Na-HEPES pH 7.5, for 15 min at 37 °C causes rapid degradation of the oligonucleotide, which eliminates Qdot binding to the test line. This resulted in a marked and quantifiable decrease in the ratio of the test line signal to the control line signal (T/C ratio). Pretreatment of RNA oligonucleotides with RNase A for one minute also caused a substantial, albeit lower, decrease in the T/C ratio (data not shown). To optimize the reaction buffer, we varied several parameters, including buffer type, pH, salt, and detergent concentration. The HEPES and Tris buffers produced highly sensitive results. Optimal reactivity was observed within the pH range of 7.5 to 8.5 (data not shown). Additionally, the addition of certain nonionic surfactants enhances the activity. Specifically, adding the Pluronic F68 surfactant (0.5 - 1%) to the reaction buffer consistently enhanced the observed reduction in the T/C ratio, leading to improved detection sensitivity. The optimized reaction buffer consisted of 20 mM Tris-HCl (pH 8.0, 0.5% Pluronic F68, and 0.05% sodium azide. This buffer was used in all the subsequent experiments.

Effect of oligonucleotide size on LFA sensitivity

Using the optimized reaction conditions and procedure, we tested similar RNA substrates of varying sizes to identify the optimal nucleotide length for maximal assay sensitivity. Four RNA oligos of 6, 10, 17, and 30 nucleotides were synthesized. Each oligonucleotide contained a 5' FAM group and a 3' biotin group (attached via a triethylene glycol (TEG) linker). Equimolar amounts of the RNA substrate were added to each tube. The RNase-catalyzed decrease in T/C ratio increased as the size of the oligonucleotide substrate increased. The 30-mer RNA oligo produced the highest sensitivity (Figure 3), as

determined by the change in T/C ratio caused by RNase. The 17-mer oligo produced a similar T/C ratio decrease, whereas little or no ratio decrease was observed for tests performed using the 6-mer substrate at this RNase dose. Under these conditions, the observed reaction sensitivities for the substrates were 30mer ≈ 17mer > 10mer > 6 mer. Although the sensitivities of the 30mer and 17mer substrates were similar, the larger substrate was used in the subsequent experiments.

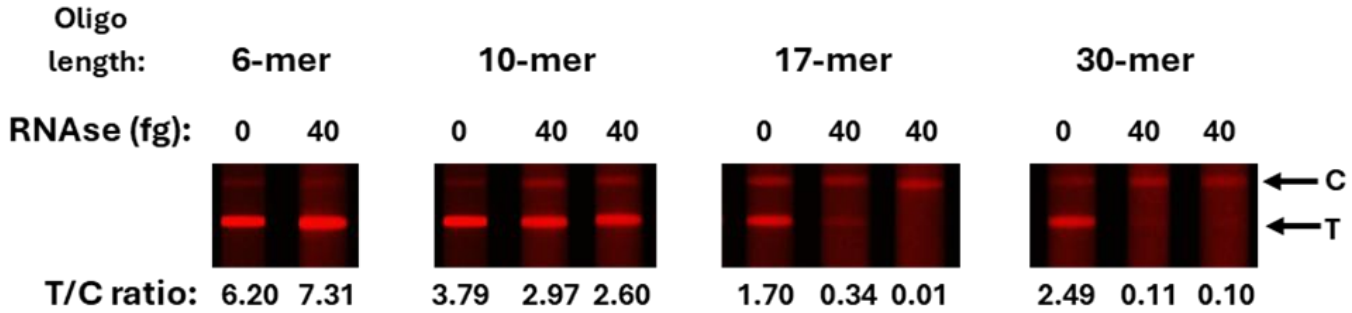

Figure 3. Effect of increasing RNA oligonucleotide size on assay sensitivity. The assay sensitivity of four dual-labeled RNA oligonucleotide substrates for detecting 40 fg of RNase A was compared using the optimized method. The oligonucleotide sizes range from 6 to 30 nucleotides as indicated. The T/C ratio for each strip is indicated.

Limit of detection and replicant variance.

To determine the detection limit, RNase A solution was serially diluted in buffer to a concentration range of 0.5 - 20 femtogram/µl (Figure 4). One microliter of each solution was tested (in duplicate) using the optimized assay. The results are shown in Figure 4. In this experiment, nearly complete substrate degradation was observed for RNase amounts of 5-20 fg, whereas only minor degradation was observed in tests using 0.5 fg. The observed RSD for the T/C ratios among the triplicate negative control tests was 17.4%. This value falls within the observed inter-day RSD range of 6 -20% for the assay. As such, the observed 94-99% reduction in the T/C ratio for all tests containing 5 – 20 fg RNase fell well outside the probable 95% confidence interval for the assay (3σ).

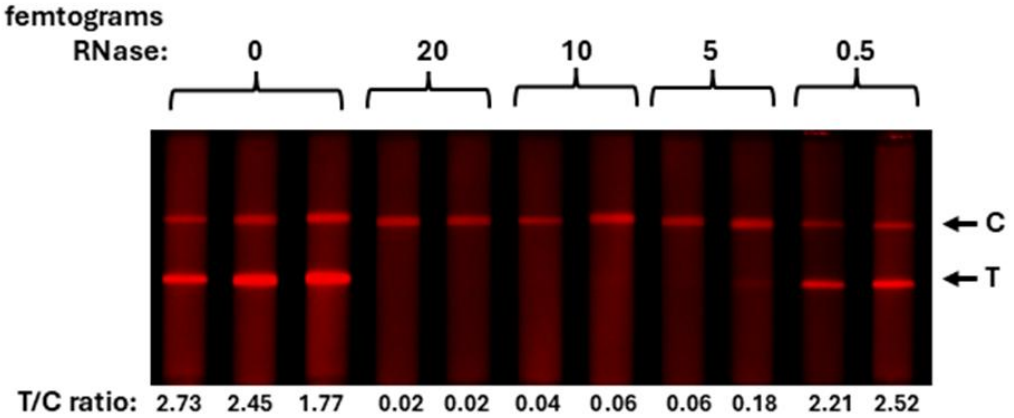

Figure 4. Rapid, ultrasensitive detection of RNase A using the optimized lateral flow assay. 1 µl replicates of serially diluted enzyme were mixed with 50 µl reaction buffer containing RNA substrate. After a 15 minute incubation, each reaction was mixed with running buffer and applied to the sample pad of the strip. The reactions flowed through the strip for 15 minutes before measuring the intensities of the test and control lines using the strip reader to calculate the T/C ratios. All RNase amounts tested, except 0.5 femtograms, cause greater than 90% cleavage of the substrate.

Detection of RNase on hard surfaces.

To test for RNase hard surfaces, we swabbed replicate 4 cm^2 glass plate sections containing 0 or 80 fg RNase A, as described in the Methods section. The nuclease was previously applied to the surface in buffer, streaked over the surface with a plastic pipette tip, and then allowed to dry for 15 min prior to swabbing. The sections were thoroughly swabbed using moistened nuclease-free cotton-tipped swabs (collection of samples using dry swabs yielded poor results). The swabs were then immersed in tubes containing reaction buffer with RNA substrate, swirled for 30 s, and incubated for 2 min before discarding the swab. Fifty microliters of each sample were then transferred to wells containing running buffer before immersion of the

strips. Nearly complete degradation was observed for RNase amounts of 80 fg, whereas no detectable degradation was observed for hard surfaces containing no RNase (Figure 5). The observed RSD for the T/C ratios among the triplicate negative control tests was 8.6%. The observed 94-96% reduction in the T/C ratio for samples containing 80 fg RNase fell well outside the probable 95% confidence interval for the assay. Tests performed using polyester or nylon swabs produced lower reductions in T/C ratios (data not shown).

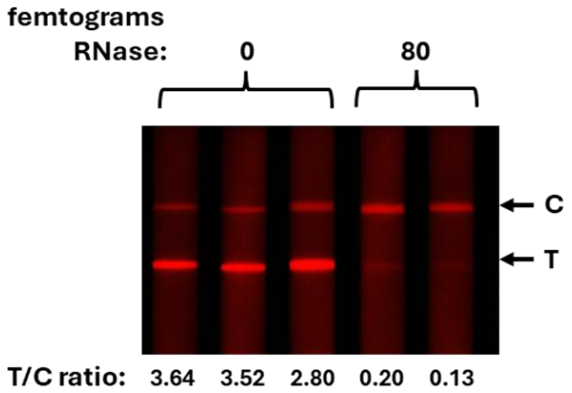

Figure 5. Convenient detection of RNase on a glass plate using the LFA test. 0 or 80 femtograms of diluted RNase A was applied to and dried onto replicate 4 cm^2 sections of glass plate. The sections were swabbed with moistened cotton swabs and introduced to tubes containing RNA substrate in reaction buffer. Samples containing 80 femtograms of RNase A caused nearly complete cleavage of the RNA substrate.

Detection of other nucleases.

To explore the versatility of the assay, we tested its ability and sensitivity in detecting other ribonucleases. Bacterial RNase I and RNase T1 were serially diluted in their respective optimal storage buffers, as recommended by their suppliers) and tested using the same RNA substrate and reaction buffer used to detect RNase A. The incubation time, temperature, and running buffer were identical to those of RNase A (Figure 6A). The results indicate that the test can detect either ribonuclease (RNase I: 0.001 units (=4 ng); RNase T1:1 unit (=87 ng); communication from suppliers). Next, we tested several nucleases (Micrococcal nuclease, Mung Bean nuclease, Benzonase, and Denarase High Salt) which contain both RNase and DNase activities, using the same procedure (Figure 6B). These enzymes were serially diluted in their respective dilution buffers and then diluted 50-fold in reaction buffer to perform the tests. Because these nucleases cleave the control DNA oligonucleotide, leading to an invalid test, we included a dual-labeled (DIG/Biotin) polyethylene glycol (PEG) linker instead of the normal DNA control oligo to facilitate control line formation. The dual-labeled PEG molecule was resistant to nucleases. We also added 1 mM MgCl2 to the reaction buffer since Mg+2 ion is an essential cofactor for these nucleases. Under these conditions, the test can detect the activity of each nuclease at the indicated sample concentration (Micrococcal nuclease: 0.01 unit; Mung bean nuclease: 1 unit; Benzonase: 1 unit; Denarase High Salt: 3 units). When using a biotin/FAM-labeled DNA substrate, the test can also detect the activity of DNase enzymes, including DNase I (data not shown).

Discussion

Our novel quantum dot-based assay permits rapid detection of extremely low amounts of ribonuclease in samples. Our work demonstrates that lateral flow assays are an ideal platform for the convenient, highly sensitive, and rapid detection of ribonucleases. The sensitivity of our assay was similar to that of the overnight gel electrophoresis assays using radioisotopes. In addition to its high sensitivity, our assay is highly reproducible, with typical RSD values ranging from 6% to 20% for nuclease-free buffer samples, which are well below the typical acceptance criteria thresholds for RNase testing assays [36]. The sensitivity of our rapid assay (RNase A LOD: 5 fg) far exceeds that of popular FRET-based assays without requiring a spectrofluorometer. Our 30-minute assay is more than 50 times more sensitive than commercially available tests, which require an expensive spectrofluorometer and hours to perform [22]. The sensitivity of FRET-based RNase assays can vary significantly depending on the gain settings and the optical sensitivity of individual spectrofluorometers [36]. Our test generates a control line signal that can be used to verify and normalize the sensitivity of each test, thereby ensuring more consistent results between the testing sites. In addition, our assay is portable, allowing it to be used outside the laboratory. Combined with the simplicity of the assay workflow, our assay is well suited for use in non-traditional testing environments.

We tested oligonucleotide substrates that ranged from 6 to 30 bases in length. The highest sensitivity was observed for oligonucleotides longer than 10 nucleotides. In contrast, lower reactivity was noted for oligonucleotides shorter than 10 nucleotides. This finding is somewhat surprising, as short dual-labeled oligonucleotides (5-10 nucleotides) are reported to be excellent RNase A substrate controls [43 -45], with their reactivity limited only by diffusion and kcat/Km values exceeding 1 x 10^9 $M^{-1}sec^{-1}$. Since Qdots are not added until the completion of the 15-minute reaction, it is highly unlikely that the lower reactivity observed for shorter oligonucleotides is due to steric obstruction of the enzyme-substrate complex.

Conversely, it is possible that as the size of the RNA substrate increases, the intact substrates bind more slowly to the Qdots, leading to preferential binding of the cleaved products. The higher detection limits observed for bacterial RNase I and fungal RNase T1 likely reflect their lower overall catalytic efficiencies than RNase A. However, it may also be possible to identify other higher sensitivity substrates for these specific nucleases.

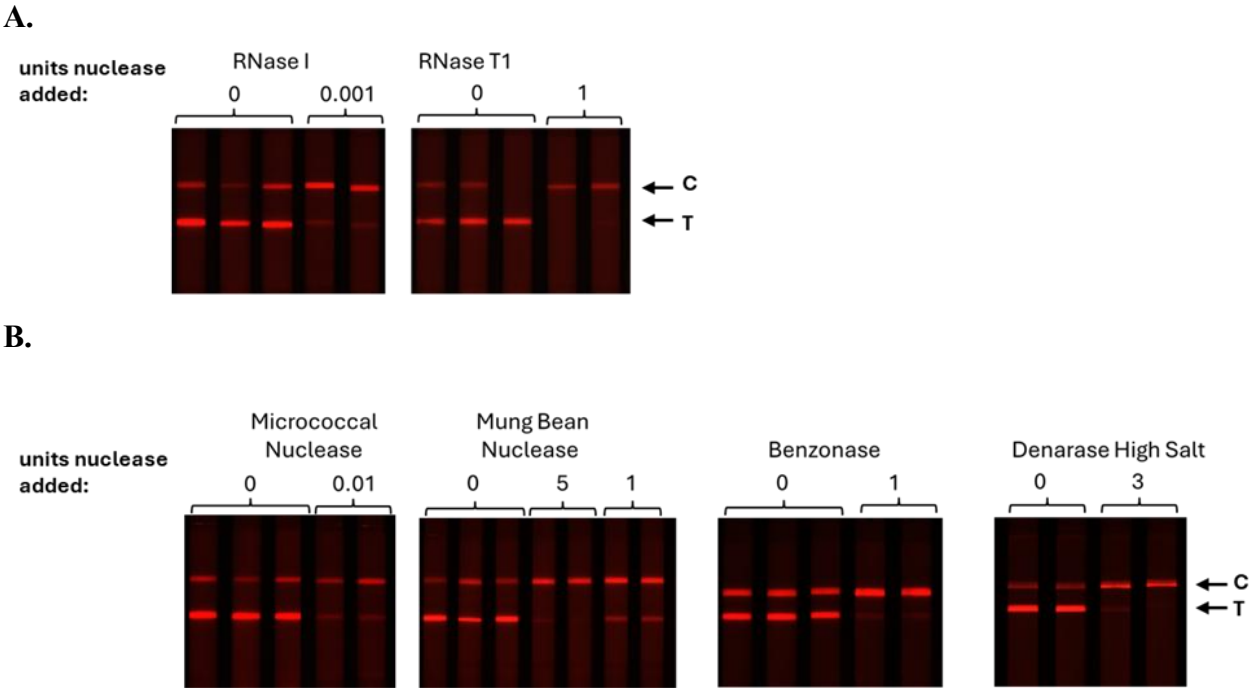

Figure 6. Detection of various RNA-cleaving nucleases using the lateral flow assay. One microliter of dilution buffer containing the indicated units of each enzyme was mixed with 50 µl reaction buffer containing RNase substrate to initiate each reaction. A. Nucleases which cleave RNA. B. Nucleases which cleave DNA and RNA.

Our test is versatile and can be readily adapted to detect nucleases such as Benzonase or Denarase. Oligonucleotide substrates are currently designed to detect nucleases capable of cleaving single-stranded RNA. By modifying the substrate composition, it is possible to detect enzymes that cleave double-stranded RNA or DNA oligonucleotides. Additionally, by altering the oligonucleotide sequence, the test can potentially be used to detect specific nucleases, such as sequence-specific endonucleases.

Our test can also be used for convenient detection of RNase on hard surfaces. We developed a swab-based system to transfer RNase contaminants from the surfaces to reaction tubes. It could readily detect less than 100 fg of dried RNase A spiked onto glass (Figure 6). The observed decrease in RNase A detection sensitivity for the swab test (80 fg) compared to that for the liquid test (5 fg) can be partially attributed to the higher liquid sample volume used for the assay (300 µL versus 50 µL). Nevertheless, this method is simple and more sensitive than any other commercially available RNase-detection system. Further testing using other surface types is ongoing in our laboratory.

References

1. Kairuz D, Samudh N, Ely A, Arbuthnot P, Bloom K. 2022. Front Immunol. 13**:** 1018961.
2. Uddin MN, Roni MA. 2021. Vaccines. (Basel) 9: 1033.
3. Meyer RA, Trabulo SM, and Douthwaite JA, Santos JL. 2022. In *Messenger RNA therapeutics* (eds. Jurga S, Barciszewski J), pp. 1-16. Springer. Cham, Switzerland.
4. Wadhwa A, Aljabbari A, Lokras A, Foged C, Thakur A. 2020. Pharmaceutics 12: 102.
5. Rcheulishvili N, Mao J, Papukashvili D, Liu C, Wang Z, Zhao J, Xie F, Pan X, Ji Y, He Y, et al. 2023. Int J Biol Macromol 226: 885-899.
6. Wang M, Zhao J, Jiang H, Wang X. 2022. Mater Horiz 9: 1111-1140.
7. Forbes TA, Brown BD, Lai C. 2021. Br J Clin Pharmacol 88: 2525-2538.
8. Berger S, Lächelt U, Wagner E. 2024. Proc Natl Acad Sci USA 121:e2307799120.

9. Lee KH, Song J, Kim S, Han SR, Lee SW. 2023. Front Mol Biosci 10: 1229246.
10. Camperi J, Lippold S, Ayalew L, Roper B, Shao S, Freund E, Nissenbaum A, Galan C, Cao Q, Yang F, *et al.* 2024. Anal Chem 96: 3886–3897.
11. Guimaraes GJ, Kim J, Bartlett MG. 2024. Characterization of mRNA therapeutics. Mass Spectrom Rev 43:1066-1090. doi:10.1002/mas.21856
12. Huang D, Li N, Dong X. 2024. Biologicals 88: 101799.
13. Servais MD, Galtier F, Nouvel A, Rebuffat S, Laget J, Géan A, Provost N, Lorcy F, Rigau V, Couderc G, et al. 2022. PloS One 17: e0278780.
14. Gaignaux A, Ashton G, Coppola D, De Souza Y, De Wilde A, Eliason J, Grizzle W, Guadagni F, Gunter E, Koppandi I, et al., 2016. Biopreserv Biobank. 14: 429-439.
15. Talu CK, Toper MH, Şahin Y, Erdoğdu İH. 2020. Turk Patoloji Derg 36: 93-108.
16. Coppola L, Cianflone A, Grimaldi AM. 2019. J Transl Med 17: 172.
17. Oude Blenke E, Örnskov E, Schöneich C, et al. 2023. J Pharm Sci 112: 386-403.
18. Whitley J, Zwolinski C, Denis C. 2022. Transl Res 242: 38-55.
19. Chang D, Chang T, Salena B, Li Y. 2020. Chembiochem 21: 464-468.
20. Rosenberg HF. 2008. J Leukoc Biol 83: 1079-1087.
21. Dean JM, DeLong RK. 2015. Methods Mol Biol 1297: 187-196.
22. Van Pottelberge R, Matthessen R, Salem S, Goffin B, Oien N, Bharti P, Ripley D. 2025. J Pharm Sci 114: 1520-1528.
23. Green MR, Sambrook J. 2019. Cold Spring Harb Protoc 2.
24. Rosa SS, Prazeres DMF, Azevedo AM, Marques MPC. 2021. Vaccine 39: 2190-2200.
25. Rosa SS, Nunes D, Antunes L, Prazeres DMF, Marques MPC, Azevedo AM. 2022. Biotechnol Bioeng 119: 3127-3139.
26. Knezevic I, Liu MA, Peden K, Zhou T, Kang H-N. 2021. Vaccines 9: 81.
27. Webb C, Ip S, Bathula NV, Popova P, Soriano SKV, Ly HH, Eryilmaz B, Nguyen Huu VA, Broadhead R, Rabel M, et al. 2022. Mol Pharm 19: 1047-1058.
28. Strom SP. 2019. Methods Mol Biol 1897: 345-357.
29. Scadden AD, Naaby-Hansen S. 2001. Methods Enzymol 341: 126-141.
30. Blank A, Sugiyama RH, Dekker CA. 1982. Anal Biochem 120:267–275.
31. Greiner-Stoeffele T, Grunow M, Hahn U. 1996. Anal Biochem 240: 24–28.
32. Saxena SK, Rybak SM, Davey RT Jr, Youle RJ, Ackerman EJ. 1992. J Biol Chem 267: 21982-21986.
33. Ye Y, Wen W, Xiang Y, Qi X, La Belle JT, Chen JJ-L, Wang J. 2008. Electroanal 20: 919–922.
34. Sato S, Takenaka S. 2013. Electroanal 25: 1652–1658.
35. Mommaerts K, Sanchez I, Betsou F, Mathieson W. 2015. Anal Biochem 479: 51-53.
36. Henry E, Charalambous E, Betsou F, Mathieson W. 2024. Heliyon: 10: e24603
37. Omidfar K, Riahi F, Kashanian S. 2023. Biosens 13: 837.
38. Zrazhevskiy P, Dave SR, Gao X. 2014. Part Part Syst Charact 31: 1291-1299.
39. Zheng S, Yang X, Zhang B, Cheng S, Han H, Jin Q, Wang C, Xiao R. 2021. Food Chem 163: 130400.
40. Jia J, Ao L, Luo Y, Liao T, Huang L, Zhuo D, Jiang C, Wang J, Hu J. 2022. Biosens Bioelectron 198: 113810.
41. Dubrovsky T. 2009. Intl J Nanosci 8: 163-167.
42. Abrams B, Dubrovsky T. 2007. Methods Mol Biol 374: 185-203.
43. Park C, Raines RT. 2001. J Am Chem Soc 123: 11472-11479.
44. Park C, Raines RT. 2003. Biochem 42: 3509-3518.
45. Kelemen BR, Klink TA, Behlke MA, Eubanks SR, Leland PA, Raines RT. 1999. Nucleic Acids Res 27: 3696-3701.